

Research Article

<https://doi.org/10.1631/jzus.A2200060>



Coordinated deformation control technologies for the high sidewall–bottom transfixion zone of large underground hydro-powerhouses

Qi-xiang FAN^{1,2✉}, Zhi-yun DENG³, Peng LIN³, Guo LI^{1,2}, Ji-lin FU², Wei HE²

¹China Huaneng Group Co., Ltd., Beijing 100031, China

²China Three Gorges Group Corporation, Beijing 100038, China

³Department of Hydraulic Engineering, Tsinghua University, Beijing 100084, China

Abstract: It is imperative to understand the spatial and temporal coordination deformation mechanism and develop targeted deformation control technologies for high sidewall–bottom transfixion (HSBT) zones to guarantee the stability of rock surrounding underground hydro-powerhouses under complex geological conditions. In this study, the spatial and temporal coordinated deformation control of HSBT zones was addressed from the aspects of the deformation mechanism, failure characteristics, and control requirements, and some coordinated deformation control technologies were proposed. On this basis, a case study was conducted on the deformation control of the HSBT zone of the underground powerhouse at the Wudongde hydropower station, China. The results showed that the relationship between excavation and support, and the mismatch of deformation and support of the surrounding rock mass in the HSBT zone of underground caverns with a large span and high in-situ stress can be appropriately handled. The solution requires proper excavation and construction procedures, fine blasting control, composite and timely support, and real-time monitoring and dynamic feedback. The technologies proposed in this study will ensure the safe, high-quality, and orderly construction of the Baihetan and Wudongde underground caverns, and can be applied to other similar projects.

Key words: Underground powerhouse; Coordinated deformation mechanism; High sidewall–bottom transfixion (HSBT); Cavern group; Control technology


1 Introduction

China has the most abundant water power resources worldwide, and Southwest China has become the center of hydropower development (Li HB et al., 2017; Lin et al., 2019; Fan et al., 2020, 2021a). The geological and hydrological conditions in western areas, which feature deep valleys, steep-sloped banks, and high tectonic stress, are very complex. Many large water diversion and power generation systems are arranged inside mountains, forming complex underground cavern groups (Lin et al., 2015; Huang et al., 2020). Large-scale underground powerhouses are characterized by their large span, high sidewalls,

crossed structure, and great buried depth (Zhang and Zhang, 2009; Lin et al., 2011, 2013; Luo et al., 2015; Panthi and Broch, 2022). The Baihetan cavern span exceeds 30 m and the height can reach 80–90 m. There are three main caverns: the main powerhouse, main transformer chamber, and tailrace surge tank (Fig. 1). The following areas constitute a significant plastic deformation zone (high sidewall–bottom transfixion (HSBT) zone): (1) the elevation range of the main powerhouse to the tailrace surge tank; (2) from the downstream sidewall to the tailrace surge tank along the longitudinal direction of the hydraulic turbine sets; (3) the partition between the two hydraulic turbine sets from the transverse direction.

Note that the draft tube gate chamber can be arranged independently (Fig. 1), as in the Baihetan hydropower station, or together with the main transformer chamber, as in the Xiangjiaba hydropower station, or with the tailrace surge tank, as in the Xiluodu hydropower station, depending on the geological and

✉ Qi-xiang FAN, qx_fan@chnng.com.cn

 Zhi-yun DENG, <https://orcid.org/0000-0001-9851-6125>

Peng LIN, <https://orcid.org/0000-0003-1338-2514>

Received Jan. 30, 2022; Revision accepted Apr. 24, 2022;
Crosschecked May 27, 2022

© Zhejiang University Press 2022

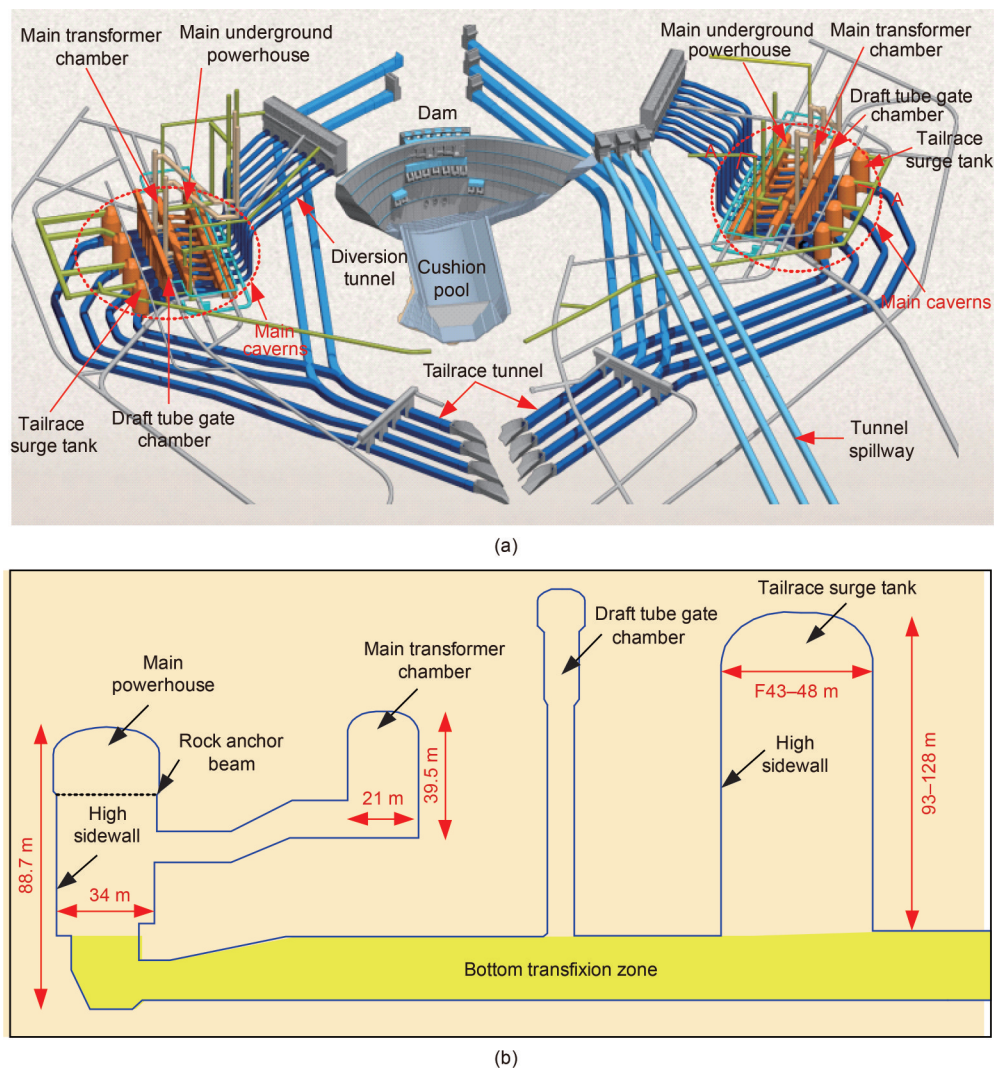


Fig. 1 Diagram of the three main caverns and the HSBT zone in the Baihetan hydropower station: (a) underground caverns in the Baihetan hydropower station; (b) three main caverns and the HSBT zone (section A-A)

topographical conditions and security calculation analysis. With the layout of the main powerhouse, the tailrace surge tank can also be replaced by a tail-water tunnel with a variable top height and its auxiliary system.

These HSBT zones control the overall safety of the underground cavern and the rhythm of the transition from excavation to subsequent installation of hydraulic turbine sets and concrete pouring. The deformation control of the HSBT zones is the priority to ensure the safety of the cavern group after the top arch is formed. Therefore, it is vital to correctly understand the time-dependent deformation mechanism and control the stability of the surrounding rock in the HSBT zones of underground powerhouses subjected

to high in-situ stress (Wang et al., 2016; Li et al., 2018, 2020; Luo et al., 2020).

Many studies have shown that deformation of the rock surrounding the large-span high sidewall under high in-situ stress conditions is a serious problem (Ghorbani and Sharifzadeh, 2009; Rezaei and Rajabi, 2018; Menéndez et al., 2019; Pinheiro et al., 2021; Kumar and Saini, 2022). For example, the integrity of the surrounding rock is relatively good at the Jinping I (Wu FQ et al., 2010; Wu AQ et al., 2016), Xiluodu, and Xiangjiaba hydropower stations (Fan and Wang, 2010; Fan et al., 2011, 2012b; Shi et al., 2018). However, sidewall deformation during the construction process was large, with non-convergent horizontal displacements or a long convergence period (Zhu et al.,

2010; Zhang et al., 2021). The spatial effect of the disturbance and failure of the surrounding rock caused by the unloading induced by excavation and the unfavorable geological plane is the primary mechanism leading to the significant time-dependent deformation of a high sidewall (Wang et al., 2016; Li et al., 2020). To ensure the stability of high sidewalls, the excavation methods of short footage, weak blasting, timely supporting, safety monitoring, and dynamic support design (Li et al., 2018, 2020) are generally adopted, and a long anchor cable is adopted for reinforcement (Wang et al., 2016; Luo et al., 2020). These methods have been successfully applied in the routine construction procedures of top-down, layer-by-layer digging, layer-by-layer anchoring, and shotcreting, as in the Xiluodu hydropower station underground powerhouse (Luo et al., 2015; Huang et al., 2022). However, in the actual construction process, due to changes in the geological environment, negligence of management, and other reasons, the excavation of an underground powerhouse may not follow the typical preset sequence (Ma et al., 2020; Shi et al., 2022). The time-dependent deformation and control technology of high sidewalls need further study. Previous studies have shown that the key factors affecting the deformation and failure of the bottom transfixion zone of an underground powerhouse are the cavern layout and structure, and the engineering geological characteristics of the rock mass (Dong et al., 2011; Wang et al., 2020). Hence, the corresponding support control measures are often different due to complex lithology, rock mass structure, in-situ stress, cavern structure, and tunnel excavation. For a single underground cavern, the failure modes of surrounding rock in underground engineering are block instability, fracture, fault slip, and bending failure (Hoek and Brown, 1980; Li et al., 2014; Song et al., 2016). For the large underground cavern groups, the failure of the surrounding rock mass can be divided into three types: structural control, stress control, and structure-stress combined control types (Dong et al., 2011; Sun YP et al., 2021). The digital control measures for a large underground cavern group were taken based on the classification system of 18 typical surrounding rock failure modes at three levels of control factors, failure mechanisms and occurrence conditions, and corresponding engineering stability analysis methods (Jiang Q et al., 2019). Targeted engineering prevention

and control measures can include layered, sequence, step excavation (Chen YF et al., 2015), excavation sequence optimization (Wu et al., 2010), surrounding rock stability geological feedback, monitoring feedback and numerical feedback (Ghorbani and Sharifzadeh, 2009; Ishida et al., 2014; Huang et al., 2020; Wen et al., 2020), real-time monitoring, and dynamic support design (Li et al., 2013; Dai et al., 2016).

Generally, research has focused mainly on the stability of a single cavern with relatively simple geological conditions. Nowadays, research on the stability of underground caverns is receiving increasing attention (Dai et al., 2016; Xiao et al., 2016; Zhou et al., 2019; Jiang et al., 2020). However, research on coordinated deformation control technologies of the HSBT zone of large underground hydro-powerhouses is still limited. For the stability control of HSBT zones of an underground powerhouse during the excavation process, other than the excavation scope, more attention should be paid to the coordinated relationship of the spatio-temporal deformation between underground caverns (Hu et al., 2018; Wang et al., 2019, 2020). First, the reasonable spacing between the caverns and the structural form of the HSBT zones should be analyzed. Second, it is necessary to study the relationship between the construction sequence, the supporting system, and the construction progress. Therefore, in this study, based on a systematic analysis of the deformation and failure characteristics and control requirements of the HSBT zone of an underground powerhouse, the control of the stability of rock surrounding the HSBT zone of a large-scale underground powerhouse under a high in-situ stress environment is discussed. The deformation characteristics and characteristics of the surrounding rock under the combined action of various factors are revealed. Technologies for controlling the mass deformation of rock in HSBT zones are also proposed.

2 Deformation characteristics, mechanism, and control requirements

2.1 Deformation characteristics of the HSBT zone

Several failure types of rock surrounding the HSBT zone in existing large-scale underground powerhouses during the construction period have been summarized (Li et al., 2020; Luo et al., 2020). They

include surrounding rock cracking and fragmentation, swelling or spalling of the concrete spray layer, deformation or cracking of the anchor head rock, dislocation of the rock anchor beam along with the expansion joint, and water seepage (Fig. 2).

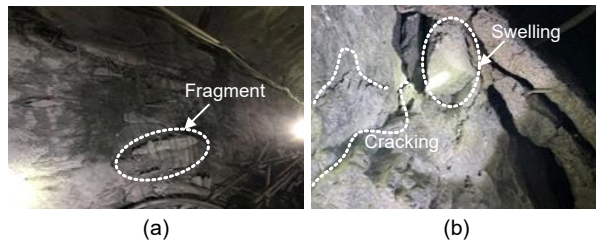


Fig. 2 Failure types of rock surrounding the HSBT zones in the Yingliangbao underground powerhouse: (a) fragment damage; (b) swelling and cracking of the concrete

It is acknowledged that the deformation and failure of surrounding rock are closely related to the high intermediate principal stress, which leads to the failure of the internal rock mass and the stress-driven deformation and failure phenomenon (Wang et al., 2016; Li et al., 2018). The deformation of the surrounding rock mass of an HSBT zone is space- and time-dependent. Typical time-displacement curves of the HSBT zone of a large-scale powerhouse are shown in Fig. 3. The deformation of the rock mass of the HSBT zone shows a sudden increase and a significant deformation rate during the blasting excavation stage, mainly due to the high stress of the surrounding rock. The rapid excavation-induced unloading in the high confining pressure environment leads to the sudden loosening and cracking of the surrounding rock, resulting in sizeable initial deformation.

After excavation and support, the engineering disturbance intensity weakens, the stress field redistri-

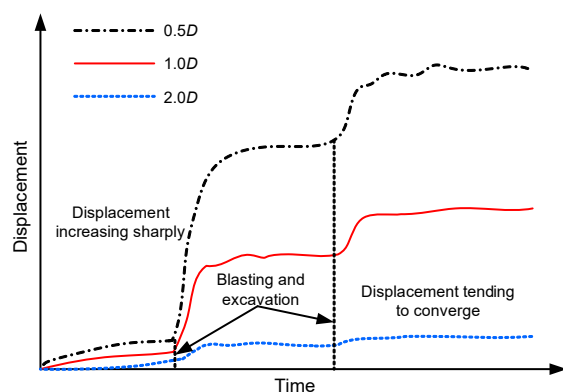


Fig. 3 Typical time-displacement curves of HSBT zones (D denotes the tunnel diameter)

bution process of the surrounding rock gradually becomes stable, and the deformation rate of the loose rock mass changes from high to low until it reaches convergence. From the perspective of space, rock deformation of an HSBT zone is the mechanical response of a rock mass subjected to excavation. The deformation involves mainly the tensile displacement of the discontinuous rock along a fracture in the loosening zone. Therefore, along the direction of spatial depth, the monitoring deformation development rules are different for monitoring points at different distances from the excavation surface due to the different degrees of rock mass looseness nearby. The closer to the excavation face, the greater the sidewall displacement (Fig. 3): the sidewall displacement at $0.5D$ is significantly higher than that at $2.0D$ away from the tunnel face.

The spatial-temporal rock deformation of the HSBT zone is one of the key factors to control to ensure the stability of an underground cavern. The time-dependent rock deformation of HSBT zones is caused by the spacing effect of stress induced by excavation changing the environment from high pressure to low confining pressure and high differential stress and rock cracking (Li et al., 2020).

Fig. 4 is a schematic diagram of the aging deformation mechanism of a high sidewall. It shows that after blasting excavation, the natural stable equilibrium state is destroyed. The tangential stress around the cavern increases while the radial stress decreases, gradually forming an environment of low confining pressure and high differential stress under the high in-situ stress field. After excavation, the surrounding rock stress release and redistribution process are not instantaneous. The release load on the excavation face is time-dependent and most of the load is released at the time of excavation. Thus, surrounding rock deformation in the initial stage of blasting excavation increases suddenly. Then the deformation rate gradually slows until the displacement tends to converge, forming a time-dependent deformation process.

The excavation of a large-span underground powerhouse causes an extensive adjustment in the range of stress in the surrounding rock, which will affect the excavation response of a small cavern within its range of influence. It is mainly characterized by the influence of excavation on the stress and deformation of surrounding rock of the main transformer tunnel and

adjacent drainage corridor. The transfixion of cavern groups is a process of transformation from separated small cavern groups to connected large cavern groups. When the partition wall that separates two cavern groups and bears a considerable load of surrounding rock is excavated and unloaded, the distribution of stress and deformation of the surrounding rock will change dramatically. The primary effect is that the diffusion section of the main powerhouse is excavated, forming a connection with the downstream sidewall of the main powerhouse, which drastically affects the surrounding rock stress of the main powerhouse. The excavation and transfixion of the lower gate well of the draft tube gate chamber will affect the stress and deformation of the surrounding rock of the upstream main transformer chamber.

2.2 Influencing factors and control requirements

The deformations of the excavation face and affected areas have strong spatial-temporal evolution characteristics due to the cavern group's layered and partitioned construction characteristics (Hu et al., 2020; Wang et al., 2020; Wen et al., 2020). For a vast cavity, the deformation of the rock mass will continue to grow for up to 4–6 years during the long excavation period. It is characterized by the continuous evolution of growth, convergence, and stability (Jiang et al., 2017; Kumar et al., 2021). This process involves the process of redistribution of rock mass stress, which is directly expressed as the deformation of rock mass, and the change of anchorage force. It is necessary to determine the mechanical properties of the

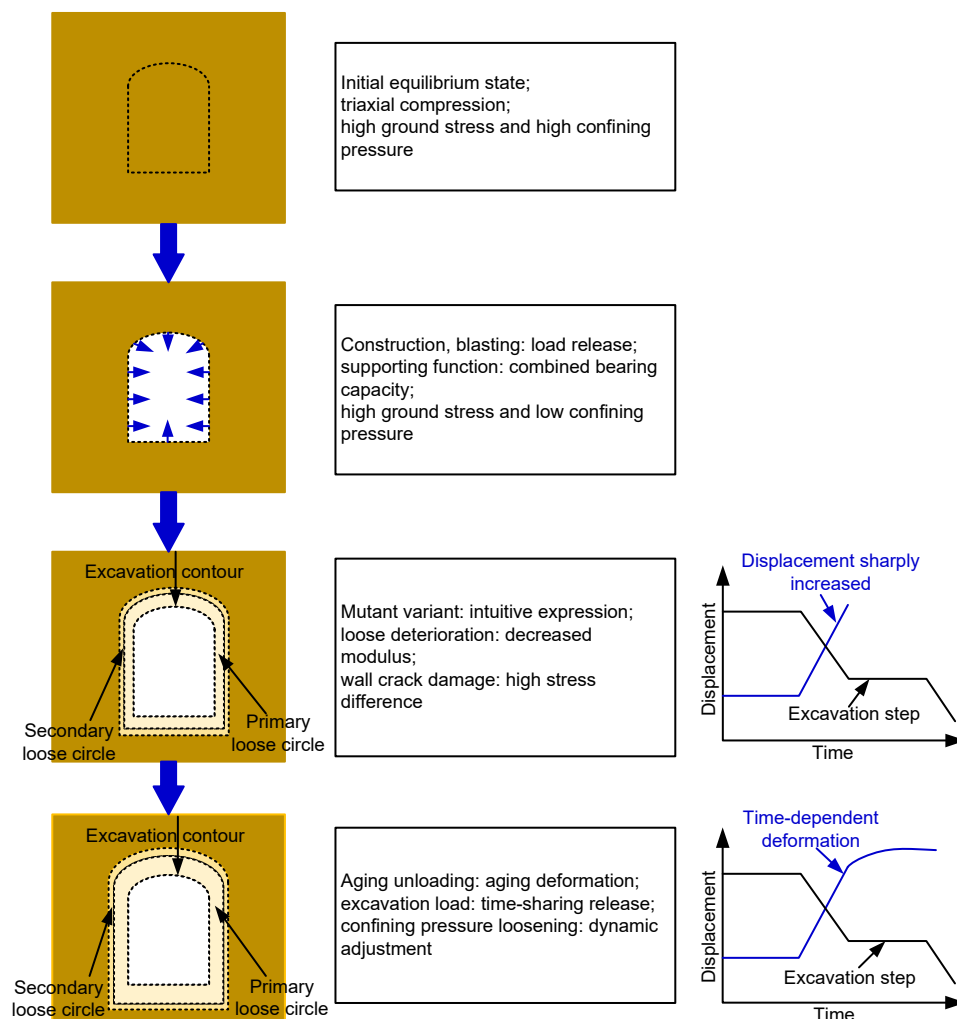


Fig. 4 Schematic diagram of the aging deformation mechanism of a high sidewall

rock mass by taking excavation and support measures. In the actual construction process, it is necessary to master the comprehensive effect of factors such as in-situ stress, rock mass characteristics, and the construction method in the complex engineering-geological environment. This can be achieved by the analysis and control of the deformation rate, deformation trend, and total deformation (Broch, 2016; Dadashi et al., 2017; Ma et al., 2020; Deng et al., 2021, 2022; Fan et al., 2021b; Sun H et al., 2021). The factors affecting the deformation of the surrounding rock are listed in Table 1.

Letting $X_1=(\sigma_{ci}; c; \varphi; \gamma; E; \nu)$, $X_2=(\text{GSI}; \text{RQD})$, $X_3=(D_0)$, $X_4=(P_i; T_i; D_i)$, and $X_5=(\text{model size}; \text{excavation sequence}; \text{boundary conditions}; \dots)$, the displacement of the surrounding rock in the large underground caverns Z_{dis} can be expressed as

$$Z_{\text{dis}}=g(X_1, X_2, X_3, X_4, X_5), \quad (1)$$

where g is the function used to obtain Z_{dis} ; X_1 indicates the material parameters; X_2 indicates the geological parameters; X_3 indicates the blast damage factor; X_4 indicates the reinforcement parameters; X_5 indicates the other parameters.

In addition, the maximum Z_{dis} ($Z_{\text{dis,max}}$) can be obtained by the following constraint conditions:

$$\begin{cases} \sigma_{ca} \leq 0.8\sigma_{ci}, \\ \sigma_{rb} \leq 0.8\sigma_{rb,\max}, \\ \sigma_{ac} \leq 0.8\sigma_{ac,\max}, \end{cases} \quad (2)$$

where σ_{ca} , σ_{rb} , and σ_{ac} are the calculated or measured maximum stress of the rock, rock bolt, and anchor cable, respectively, and $\sigma_{rb,\max}$ and $\sigma_{ac,\max}$ are the permissible

Table 1 Factors affecting the deformation of the surrounding rock in large underground caverns

Factor	Parameter	Computational formula	Note
Intact rock	Uniaxial compressive strength (UCS) σ_{ci} ; Mohr-Coulomb (MC) parameters: cohesion c and friction angle φ ; unit weight γ ; elastic modulus E ; Poisson's ratio ν	$\frac{\sigma_n}{\sigma_{ci}} = \frac{\sigma_3}{\sigma_{ci}} + \frac{\left(\frac{m_b \sigma_3}{\sigma_{ci}} + s\right)^a}{2 + am_b \left(\frac{m_b \sigma_3}{\sigma_{ci}} + s\right)^{a-1}},$ $\varphi = \arcsin \left[1 - \frac{2}{2 + am_b \left(\frac{m_b \sigma_3}{\sigma_{ci}} + s\right)^{a-1}} \right],$ $\tau = \frac{\sigma_{ci} \cos \varphi}{2 \left(1 + \frac{\sin \varphi}{a} \right)^a} \left(\frac{m_b \sigma_n}{\sigma_{ci}} + s \right)^a,$ $c = \tau - \sigma_n \tan \varphi$	σ_1 and σ_3 are the maximum and minimum principal stresses at failure, respectively; σ_n and τ are the normal and shear stresses, respectively; m_b , s , and a are the Hoek-Brown (HB) input parameters estimated from the HB constant m_i , the geological strength index (GSI), and the blast damage factor D_0 , respectively (Shen et al., 2012)
Rock mass structural characteristics	GSI; rock quality designation (RQD)	$\text{GSI} = 1.5J_{\text{cond89}} + \frac{\text{RQD}}{2},$ $J_{\text{cond89}} = \frac{35J_r/J_a}{1 + J_r/J_a},$ $\text{RQD} = \frac{\sum(\text{Length of core pieces})}{\text{Total length of core sum}} \times 100$	J_r and J_a are the joint roughness number and joint alteration number, respectively; J_{cond89} is the joint condition rating (Hoek et al., 2013)
Blast	Blast damage factor D_0	$\sigma_1 = \sigma_3 + \sigma_{ci} \left(m_b \frac{\sigma_3}{\sigma_{ci}} + s \right)^a,$ $m_b = m_i \exp \left(\frac{\text{GSI} - 100}{28 - 14D_0} \right),$ $s = \exp \left(\frac{\text{GSI} - 100}{9 - 3D_0} \right),$ $a = \frac{1}{2} + \frac{1}{6} \left(e^{\frac{\text{GSI}}{15}} - e^{\frac{20}{3}} \right)$	Hoek et al. (2002)
Reinforcement	Supporting intensity P_i ; supporting time T_i ; supporting depth D_i		
Others	Model size; excavation sequence; boundary conditions; ...		

maximum stresses of the rock bolt and anchor cable, respectively. Usually, Z_{dis} can be obtained by numerical methods based on the equilibrium equations, geometric equations, constitutive equations, and boundary conditions:

$$\begin{cases} \text{Equilibrium equations: } \sigma_{ij,j} + f_i = 0, \\ \text{Geometric equations: } \varepsilon_{ij} = \frac{1}{2}(\mu_{i,j} + \mu_{j,i}), \\ \text{Constitutive equations: } \sigma_{ij} = E_{ijkl} \varepsilon_{kl}, \\ \text{Boundary conditions: } \mu_i = \bar{\mu}_i, \quad \sigma_{ji} n_j = \bar{t}_i, \end{cases} \quad (3)$$

where $\sigma_{ij,j}$ is the surface stress tensor component; f_i is the body stress tensor component; ε_{ij} is the strain tensor; $\mu_{i,j}$ is the derivative of displacement tensor; σ_{ij} is the surface stress tensor; E_{ijkl} is the elastic modulus tensor; μ_i is the boundary values of displacement components; n_j is the boundary normal vector; $\bar{\mu}_i$ and \bar{t}_i are the known boundary values of displacement component and stress component, respectively.

In the specific case of the Baihetan underground caverns, most of the factors stated above can be determined, thus a displacement management standard can be put forward based on the numerical results, monitoring data, standard specification, and field problem characteristics (Fig. 5 and Table 2).

When the monitored change of the high sidewall or lower transfixion areas reaches a critical level, the monitoring center will issue a warning and encrypt an observation after analysis and judgment. If necessary, an on-site survey will be organized to identify the reasons, and countermeasures will be formulated.

3 Coordinated deformation control technologies

Based on the deformation and failure mechanism of rock surrounding a high sidewall, the deformation

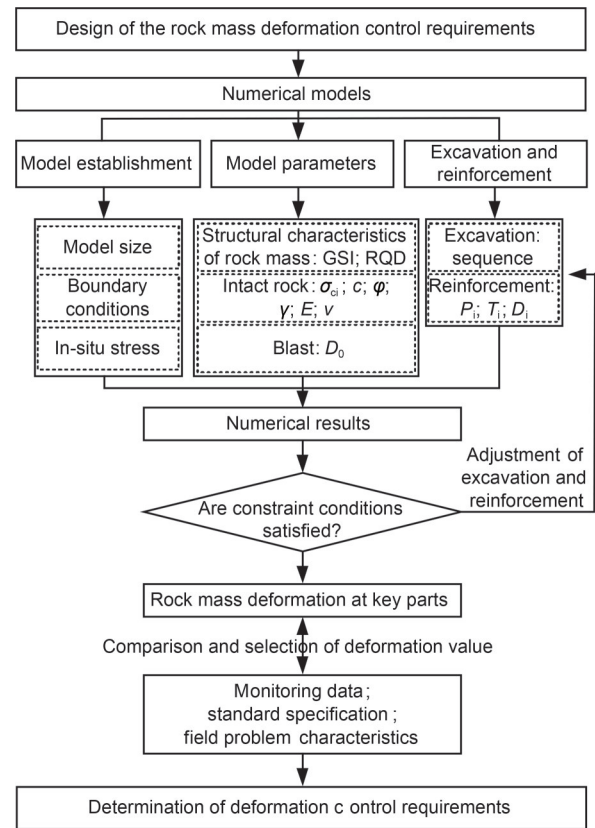


Fig. 5 Flow diagram for the determination of deformation control requirements

coordination and control technology of a typical high sidewall in China is summarized in Table 3. Due to the complexity of underground cavern groups, the current design code SL 266-2014 (MWR, 2014) does not give a clear method for controlling the stability of the surrounding rock. The code only describes the basic analysis and design principles (Kumar et al., 2021; Sun YP et al., 2021). To guide the real-time analysis and control of the local stability of rock surrounding large underground cavern groups, a coordinated control technology of deformation of underground cavern groups under normal construction conditions is summarized in Table 4.

Table 2 Control requirements for surrounding rock deformation in the Baihetan underground powerhouse

Rock grade	Safety level		Warning level		Danger level	
	Δ (mm)	δ (mm/d)	Δ (mm)	δ (mm/d)	Δ (mm)	δ (mm/d)
III	≤ 15	≤ 0.2	(15, 25)	(0.2, 1.0)	≥ 25	≥ 1.0
IV	≤ 25	≤ 0.2	(25, 35)	(0.2, 1.0)	≥ 35	≥ 1.0

Δ is the increase in deformation; deformation rate δ refers to the average deformation rate every 7 d and 24 h after blasting and unloading

Table 3 Deformation coordination and control technology of a high sidewall of a typical large-scale underground cavern

Name	Dimension of powerhouse (length×width×height) (m)	Buried depth (m)		Maximum principal stress (MPa)	Lithology	Rock mass quality grade	General deformation (mm)	Maximum deformation (mm)	Main deformation control technique
		Horizontal direction	Vertical direction						
Left bank of Baihetan	384.03×31.9×75.6	300–450	340–480	21.06	Basalt	Mainly III ₁ , minor II	50	103	Thin-layer protection excavation, quickly follow-up of support, whole-process monitoring and guidance, six-sequence fine excavation and blasting in three zones of rock wall beam layer, protective layer and rock platform (Lu et al., 2018; Wang et al., 2019; Fan et al., 2021b)
Right bank of Baihetan	438×34×88.7	420–800	420–540	30.99	Basalt	Mainly III ₁ , minor III ₂			
Left bank of Wudongde	333×32.5×89.8	75	160–540	11.6	Limestone, marble, dolomite	Mainly II, III	24	58	Carbonaceous film area, weak blasting, deep anchoring, buttress wall, rigid-flexible support plus grouting, weak blasting, tight anchorage, anti-relaxation
Right bank of Wudongde	333×32.5×89.8	66	210–390	8.2					
Nuozhadu	25.75×74.1	627–700	–	13.2	Granite, sedimentary rock	–	6	14	Fine geological exploration, complex rock and soil modeling analysis (Wang and Shao, 2010; Lv and Chi, 2018)
Pengshui	252×30×84.5	130–200	–	10	Calcareous shale	IV	15	43	Thin layer excavation, pre-stressed anchorage, consolidation grouting reinforcement without cover weight, pre-stressed rock anchor beam without crack (Liu, 2010)
Xiangjiaba	255.4×33.4×85.2	130	120–240	12.2	Sandstone	Mainly II, minor III	30	65	Pre-split blasting (Fan et al., 2011; Jing et al., 2015)
Ertan	280.3×30.7×65.4	300	200–300	38.4	Syenite, basalt	–	40	104	Reinforcement of long anchor cable (Zhu et al., 2007)
Longtan	388.8×30.3×74.5	–	100–280	28	Black cloud granitic gneiss	Mainly II–III	40	83	Short footage, weak blasting, timely support (Gan et al., 2019)
Jinping II	276.99×28.9×68.8	110–300	180–350	35.65	Marble	Mainly III	60	94	Timely support, blasting control, safety monitoring, and dynamic design of support (Chen et al., 2011)

Table 4 Deformation coordination and control technology of underground cavern group cases

Name	Size of tailrace surge tank (m)	Dimension of main transformer chamber (length×width×height) (m)	Main geological problem	Lithology	Average deformation (mm)	Maximum deformation (mm)	Main deformation control technique
Baihetan	$\Phi(43-48) \times (93-128)$	$368 \times 21 \times 39.5$	High in-situ stress, brittle basalt, weak interbedded dislocation zone	Basalt	90	192	Advanced and pre-control, thin vertical layering, fine plane zoning, short step length, fine blasting, fast and strong support, full-time measurement, dynamic inversion optimization (Fan et al., 2018; Lu et al., 2018; Han et al., 2019; Wang et al., 2019)
Wudongde	$\Phi 53 \times 113.5$	$272 \times 18.8 \times 35$	Large range of carbonaceous thin film area, steep small angle stratified rock mass	Limestone, marble, dolomite	40	72	Meter-level survey, spatial and temporal layout optimization design, system perception, parameter inversion, closed-loop control system, personalized support reinforcement, fine excavation control (Hu et al., 2018)
Lianghekou	$190.0 \times 19.5 \times 80.4$	$239.4 \times 18.8 \times 25.3$	High altitude, high cold, high ground stress, rock burst	Sandstone, metamorphic siltstone, silty slate	25	54	Drainage ahead, thin layer excavation, layer by layer support (Jiang X et al., 2019; Xiao et al., 2019)
Ertan	$203 \times 19.8 \times 69.8$	$214.9 \times 18.3 \times 25$	High ground stress	Syenite, basalt	50	124	Stratification, sequence and step excavation (Chen F et al., 2015)
Longtan	$95.3 \times 21.6 \times 89.7$	$397 \times 19.5 \times 22.5$	Steep dip stratified rock mass	Black cloud granitic gneiss	45	97	Real-time monitoring and dynamic design of support (Jin et al., 2009)
Xiluodu	$317 \times 95.0 \times 25.0$	$349.3 \times 33.32 \times 19.8$	Interbedded dislocation zone of basalt formation	Basalt	30	60	Monitoring feedback and numerical feedback (Fan and Wang, 2011; Fan et al., 2012a; Huang et al., 2022)
Jinping II	$192.3 \times 26.3 \times 23.9$	$374.6 \times 19.8 \times 31.4$	High in-situ stress, steep dip stratified rock mass, local brittle failure	Marble	20-60	>100	3D numerical simulation, dynamic optimization of excavation and support (Wu et al., 2010)
Laxiwa	$\Phi 29.6 \times 113.5$	$354.75 \times 29.0 \times 53.0$	High ground stress and brittle failure	Granite	30-40	60-70	Cracking-suppression method, global optimization of excavation sequence (Jiang Q et al., 2019)

Tailrace surge tanks of Baihetan and Laxiwa are cylindrical (Φ indicates the diameter), and that of Wudongde is semi-cylindrical

With the gradual increase of the size of the HSBT zones of an underground powerhouse, a single control technology is gradually transformed into a comprehensive construction technology. With the geological information, support scheme and monitoring results of on-site excavation, the back analysis, and simulation of the excavation deformation of the underground space structure can be carried out in time, and support design and construction measures can be simultaneously adjusted. The relevant parameters of ground stress and rock mass mechanics are inverted by comparing each layer's predicted and measured deformation values after excavation. Thus, the geological model and the layered and sequential excavation model are continuously updated to optimize the design and construction measures, predict the subsequent excavation response, and improve the effectiveness of the excavation support measures.

3.1 Proper excavation and construction procedures

Adopting the idea of a 3D, multi-level, and planar multi-process, the construction procedures and the excavation layout of each layer of a powerhouse are considered and planned as a whole. In particular, the construction procedures of the access tunnel entering the powerhouse are taken into account in advance. Taking the powerhouse on the right bank of the Wudongde hydropower station as an example (Fig. 6), the excavation procedure is as follows: the top arch of the main-transformed cavern is excavated after the excavation of arch crown I. After the excavation and support of layer I, the excavation of layer II should be completed as soon as possible. After the temporary support of the layer II sidewall is completed, the channel is formed by slotting downstream of layer III of the main-transformed cavern to excavate the access tunnel as soon as possible. The access tunnel excavation and the lock support of the powerhouse side are completed in sequence according to the sequence of interval and jump cavern excavation to realize the excavation target of “cavern first and high sidewall follows”. This is conducive to the rapid construction of the next part and the rock anchor beam, and the stability of the powerhouse high sidewall.

In the HSBT zones, a special scientific and reasonable excavation construction procedure is adopted

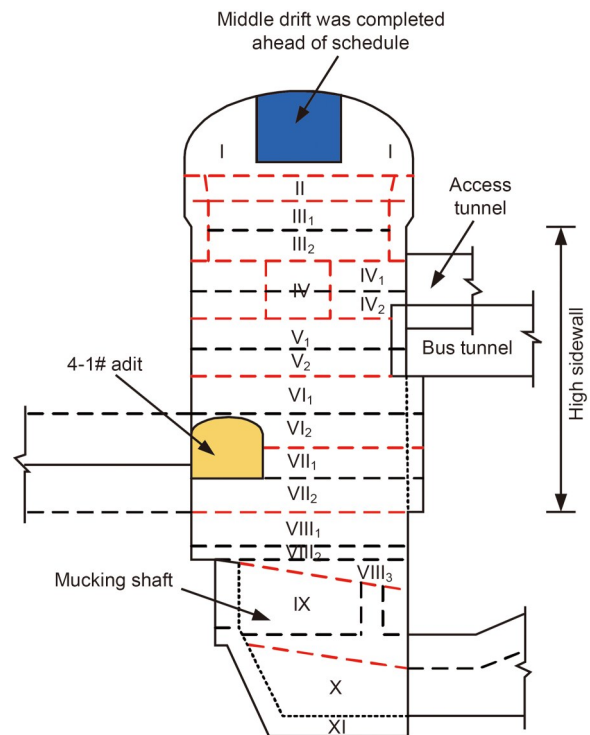


Fig. 6 Schematic diagram of the excavation procedure of the main powerhouse on the right bank of the Wudongde project

according to the spatial characteristics of the cavern structure and the principle of stable sidewall formation. Firstly, the excavation and support construction of the small cavern is carried out. Then, the small cavern penetrates 10–20 m into the high sidewall area of the cavern. After that, the excavation and connection of the high sidewall are carried out.

The combination scheme of the excavation sequence designed by experience cannot be guaranteed to be the most reasonable for the stability of cavern groups (Hu et al., 2018; Jiang Q et al., 2019). The cavern group effect of the HSBT zones can be significantly reduced during cavern construction by adopting an optimal excavation scheme. Also, optimal excavation is helpful to reduce the unloading of one excavation to avoid the severe deformation of surrounding rock and the change in linkage of surrounding rock deformation of multiple caverns. Taking the excavation sequence of caverns of the Baihetan underground powerhouse as an example (Fig. 7), the optimal excavation scheme is as follows. First, the excavation method of “staggered time and staggered distance” is adopted. The excavation is staggered at a certain distance and a certain time interval. To reduce the

intensity of adjustment in the surrounding rock, the excavation is not performed simultaneously in the same area. Second, in the case of a small tunnel penetrating a big tunnel, the excavation method of “cavern first and wall behind” is adopted. The water diversion pressure tunnel and tail-water diffusion tunnel are excavated into the workshop first. Third, timely support should be carried out after the small tunnel penetrates the big tunnel to reduce the influence of excavation of the large tunnel on the stability of the rock surrounding the small tunnel. Combined with the existing construction technology, construction machinery, equipment, and construction channel layout, a layered excavation plan of the four main caverns is carried out from top to bottom. The main and auxiliary workshop is divided into 10 layers (Fig. 7). The main transformer tunnel is divided into five layers, the tailrace tunnel into four layers, and the tailrace surge tank into three layers.

3.2 Fine blasting control

The excavations of HSBT zones of an underground powerhouse can adopt fine blasting, fast sealing, and timely anchoring technology to ensure the cavern’s forming quality and reduce the blasting effect of the cross cavern. For example, the main powerhouse can adopt a 5–7 m kerf blasting in the middle part, and a 4 m protective layer is reserved on both

sides to expand and follow up. The protective layer adopts a mobile standard construction sample frame and smooth vertical blasting with a small aperture, small charge, and millisecond difference to reduce vibration damage to the sidewall–bottom transfixion zones. All boreholes are made by hand pneumatic drill. Single blasting dosage is strictly controlled within 20 kg. Through fine blasting technology, the ultimate forming and stability of HSBT zones are ensured. In addition, the drilling and blasting process is standardized to reduce the impact of blasting vibration and ensure the stability of the HSBT zones of the powerhouse by adopting the principle of the personnel, machine, and location positioning, and “one-battery-one-summary” quality control method.

3.3 Composite and timely support

For the particularity of discontinuous fracture depth and different degrees of fracture of surrounding rock under high stress, the general principle of support should be closed in a timely manner by spraying concrete to form surface confining pressure and a bonding effect. At the same time, anchor reinforcement is carried out in real-time to control the propagation of cracks in the shallow surrounding rock and improve the structural strength of the shallow surrounding rock. If necessary, a pre-stressed anchor

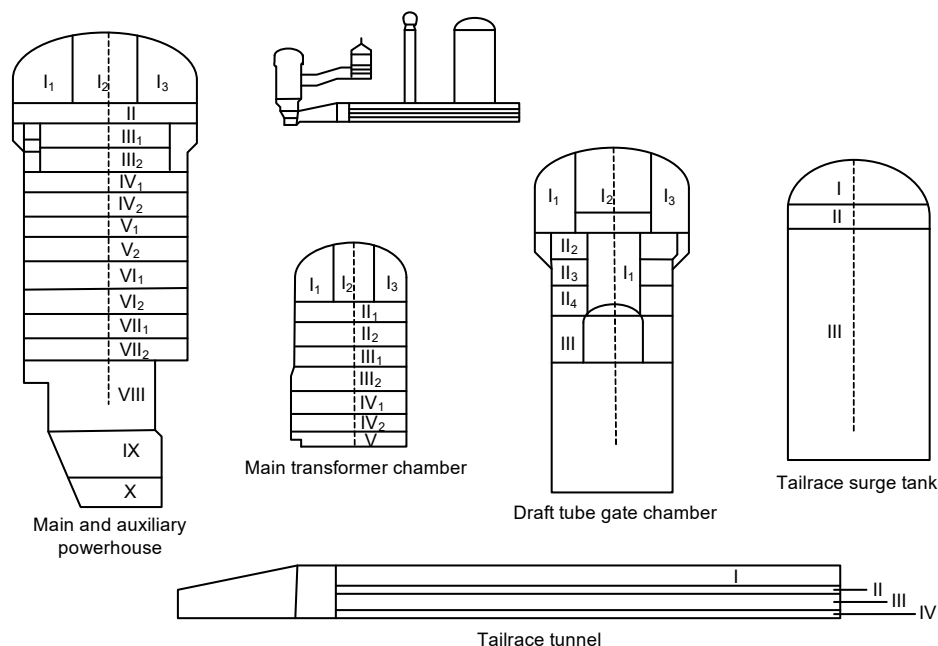


Fig. 7 Schematic diagram of the excavation and stratification of the Baihetan underground cavern group

can suppress the development of fractures in shallow surrounding rock with a large degree of cracking, and the bond strength of the fracture surface of cracked surrounding rock can be directly improved by grouting. A long pre-stressed anchor cable should be adopted for deep reinforcement to control the progressive development of internal failure of the rock mass. The surface-shallow-deep joint reinforcement method is helpful to form a relatively complete stress-bearing structure that effectively increases the strength of broken or damaged surrounding rock. Thus, the bearing performance of all the surrounding rock can be enhanced, converting the rock from a supporting structure to a bearing structure. In particular, for the cross-section into the cavern, the above measures can be taken to strengthen the support under various adverse geological conditions. For example, given the characteristics of rock surrounding a large underground cavern, such as a thin layer, steep dip angle, and weak shale geological structure, the excavation unloading deformation is fast and difficult to control. The new technology of pre-stressed hollow grouting bolt is adopted to reinforce the shallow surrounding rock in a timely manner. A steel plate anchor pier head is used instead of a concrete one to accelerate the construction progress and achieve deep anchorage. Thus, the possibility of unloading deformation in the surrounding rock is reduced, and the problem of shallow and deep anchorage of weak shale is solved (Han et al., 2019). To solve the problem that the deformation of the underground powerhouse on the right bank of Baihetan hydropower station continued to expand with the excavation of the tunnel, the construction technology of precise hole making through an anchor cable with the high sidewall was adopted. Thus, the stability of surrounding rock deformation was ensured (Wang et al., 2019). Because of the deformation and instability of the sidewall under high immediate principal stress, it is necessary to adopt appropriate deep support measures such as an anchor cable. Moreover, the deep support in this environment must have sufficient strength to provide the confining pressure necessary for surrounding rock stability (Shi et al., 2018; Zhang et al., 2018). Regarding the supporting time of the surrounding rock, the aim should be to avoid the development trend of catastrophic failure of the surrounding rock.

Referring to the previous research result (Jiang Q et al., 2019), when the support time is too late, the

failure of the surrounding rock will be aggravated under the unconstrained and high-stress drive, which will lead to excessive failure/relaxation of the surrounding rock. However, if the support is premature, the elastic deformation of the surrounding rock cannot be effectively released, which will inevitably lead to the failure of the supporting structure. In this situation, the surrounding rock support needs to resist the elastic unloading deformation of surrounding rock beyond the ultimate strength and fracture, resulting in a significant increase in the fracture/relaxation of surrounding rock. The elastic deformation of the rock mass is released only when the supporting time is reasonable and the fracture depth is within the acceptable range. In this situation, the surrounding rock support can effectively control the subsequent development of surrounding rock fracture and deformation, and maintain the working load of the supporting structure within the design value interval. When the failure depth of the surrounding rock is large, more support cost is needed to effectively control the depth and degree of failure of the surrounding rock.

3.4 Real-time monitoring and dynamic feedback

Real-time monitoring and feedback are reflected in the following aspects:

(1) Monitoring of the blasting particle vibration velocity, acoustic wave tests before and after rock blasting, and the third-party test of grouting plumpness of bolt should be carried out.

(2) Data of the change in deformation and stress of the rock surrounding the supporting structure should be obtained by embedding the multi-point displacement meter, dislocation meter, anchor bolt, and cable dynamometer in a representative section system.

(3) Further special tests on the deformation characteristics of the rock mass should be conducted to obtain the evolution of the deformation and fracture of the deep rock mass. A variety of tests should be carried out, such as borehole photography in the rock mass and microseismic monitoring.

(4) Necessary anchoring observation corridors and facilities should be added in critical parts of the cave group.

(5) The frequency of acquisition of monitoring data should be adjusted in a timely manner, and the engineering site's implementation progress and compliance with safety requirements should be monitored.

When the cavern is excavated, the deformation and failure information and the geological information of the surrounding rock are gradually enriched. The mechanical parameters of the rock of the engineering core area can be accurately obtained by indoor testing. Blasting excavation tests and support tests can provide results for optimization of excavation and support (Li X et al., 2017; Behnia and Seifabad, 2018). The monitoring data of conventional deformation, bolt stress, and cable load during cavern excavation can provide the unloading response information of the surrounding rock. The observa-

tion methods, such as multiple acoustic tests, multiple borehole photography, and real-time monitoring of space microseismic activity of surrounding rock failure in critical areas can reveal the evolution characteristics of surrounding rock unloading failure more precisely (Wu et al., 2016; Behnia and Seifabad, 2018; Kumar et al., 2021). Therefore, the stability control and support optimization of the cavern group are further improved. The implementation process and critical optimization components of cavern group deformation control are illustrated in Fig. 8.

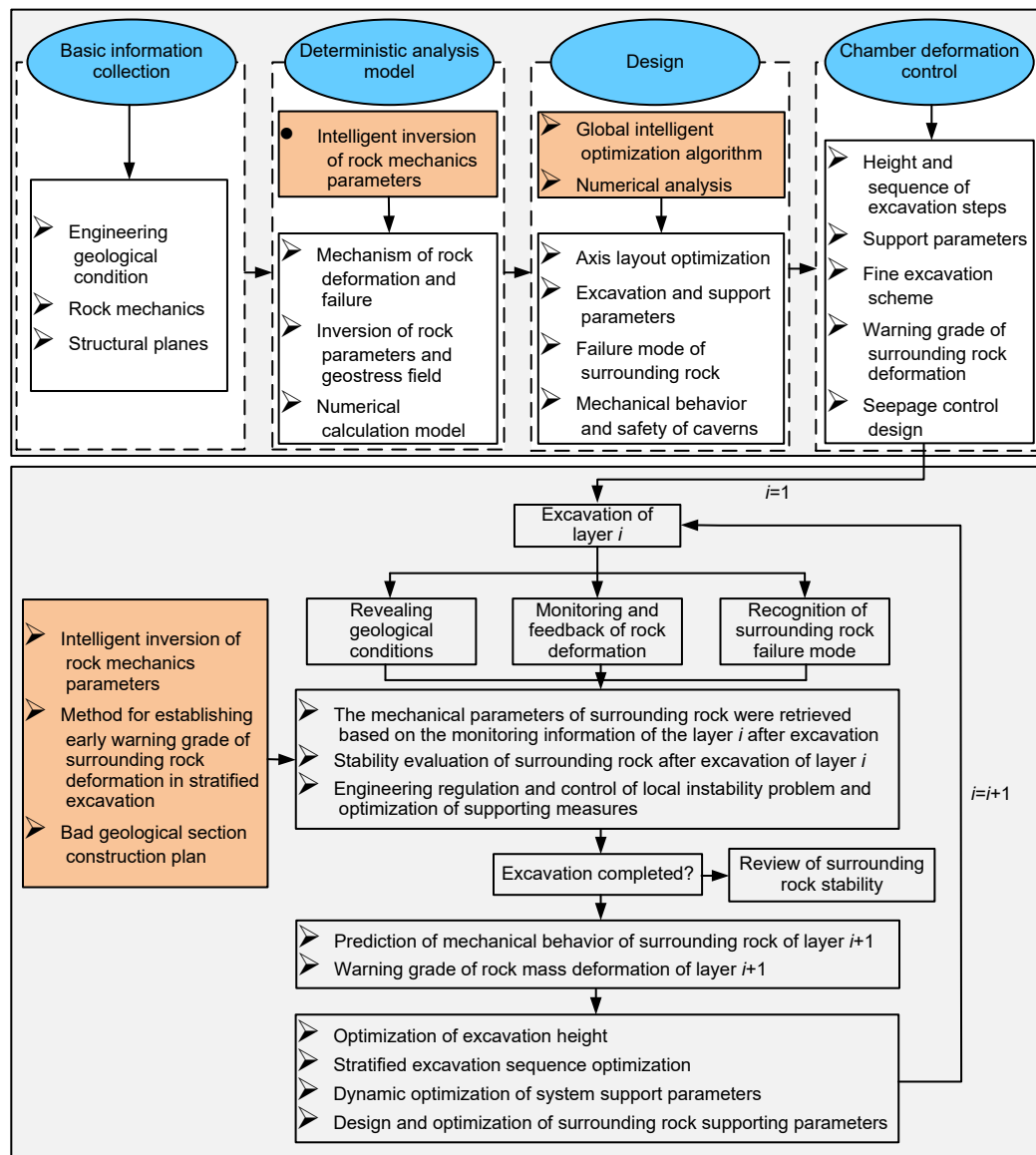


Fig. 8 Components of dynamic optimization and adjustment of deformation control of a cavern group

4 Case studies of HSBT zones

4.1 Background

The Wudongde main powerhouse on the right bank follows the excavation procedure of a 3D, multi-level, and planar multi-process. The excavation is from top to bottom, with one layer of excavation and one layer of support. The excavation section of layer I is 13.5 m×32.5 m (height×width), and the top arch is three-centered. The size of excavation of the middle pilot tunnel in the early stage is 10 m×12 m (height×width). The high sidewall below layer IV is excavated in layers from top to bottom. The high sidewall takes 6–7 m slot broaching in the middle part with 4–5 m protective layers on both sides. Layer IV is through the excavation of the high sidewall and L3 construction adit. First, the construction of the connection with L3 is performed in hydraulic turbine sets 7 and 8. The excavation methods for layers VII and VIII were the same as those for layer IV, and the layer IX, in which the vertical height from the top arch of the powerhouse is more than 70 m, was through the excavation of the machine nest and tail-water branch cavern. The rock stabilities of the high sidewall and top arch were prominent in the excavation process. Layers X and XI were machine nest and protective floor layers excavated by smooth blasting.

During the blasting construction of layer VI excavation in the main powerhouse on the right bank, the deformation of the upstream sidewall at the hydraulic turbine sets 7 and 8 increased suddenly. Deep cracking of the surrounding rock along the layer occurred, which seriously affected the overall stability of the high sidewall. In terms of local geological conditions, the abnormal deformation area is located in the area with a small angle ($<20^\circ$) between the strike of the rock layer and the axis of the powerhouse, and the rock layer has a steep dip (inclined to the downstream). The rock layer is relatively thin and smooth, the bond strength is weak, and the geological conditions are poor, which are the geological factors associated with the abnormal deformation of the upstream sidewall. In terms of construction impact, the upstream sidewall of the powerhouse formed the HSBT zone (Fig. 9) after layer VI was excavated and the L3 construction adit was connected. Stress adjustment caused the unloading relaxation of the upstream sidewall along with the rock layer. The roof blasting of

the L3 construction adit resulted in a sudden increase of 20 m in the height of the high sidewall. During the roof blasting, the actual height of the two rows of anchor cables above was not constructed, which increased by 30 m. The length of the roof blasting was 35 m and the lateral constraint was suddenly relieved, which was the mechanical factor of the abnormal deformation of the upstream sidewall.

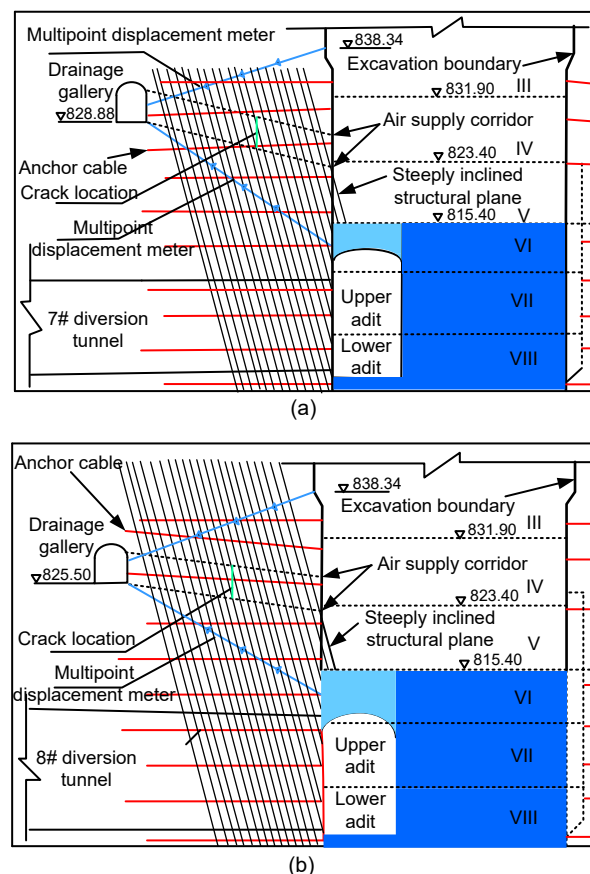


Fig. 9 Excavation of L3 construction adit at hydraulic turbine sets 7 and 8: (a) No. 7; (b) No. 8 (unit: m)

In terms of abnormal deformation of fracture morphology, the position and shape of circumferential fractures in shotcrete indicate that the deformation of the upstream sidewall towards the powerhouse's open surface after layered excavation results in tensile fractures of the surrounding rock layer at this position. Then, it leads to obvious circumferential fractures in the tunnel wall of the air supply corridor intersecting with the rock formation at a large angle. Furthermore, according to the fracture connectivity test of surrounding rock in the air supply corridor, the fractures at hydraulic turbine set 7 extend widely along

the plane direction. This indicates that the shear strength of the rock mass in this part decreases due to the plane opening and further produces the overall sliding of the surrounding rock along its plane. According to the deformation monitoring data, the abnormal deformation is mainly in the shallow surface of the surrounding rock, but the surface cracking gradually extends to the deep surrounding rock. The abnormal deformation mechanism of the upstream sidewall of the main powerhouse on the right bank is also analyzed and explained using numerical simulation (Fig. 10).

In Fig. 10 (Feng et al., 2015), the length, width, and height of the calculation model are 927, 82, and 666 m, respectively. The length is 82 m along the axis of the tunnel. The maximum buried depth of the top arch of the main powerhouse is 286 m. When the initial geo-stress field of the model was generated, the deadweight stress was the maximum principal stress. The lateral pressure coefficients along the axis and perpendicular to the axis of the vertical tunnel were 0.8 and 0.6, respectively. The upper surface of the model was a free boundary, and the other surfaces were subjected to normal constraints. Mohr-Coulomb strength criterion is adopted for rock, and the same criterion considering residual strength is adopted for the structural surface. Mechanical parameters of the rock mass and the structural surface are shown in Table 5.

Since the rock mass of layer VI constricts the lateral deformation of the main powerhouse sidewall, the maximum deformation of the surrounding rock before the excavation of layer VI concentrates around the anchor beam of the upstream sidewall. When layer VI is excavated, the upper sidewall is in lateral restraint contact, and the surface rock mass cut by the layer has the space to deform downward and toward the inside of the powerhouse. Therefore, the maximum deformation position is transferred to the lower part of the sidewall, resulting in an obvious increase in the sidewall lateral deformation (Fig. 10c).

4.2 Countermeasures and effect analysis

Abnormal deformations at hydraulic turbine sets 7 and 8 (Fig. 9) are caused by several factors including the smooth small tilt angle strata (geology), excessively long one-time exposure (construction conditions), and the excavation method of rock layer to the unloading relaxation (mechanical condition). There-

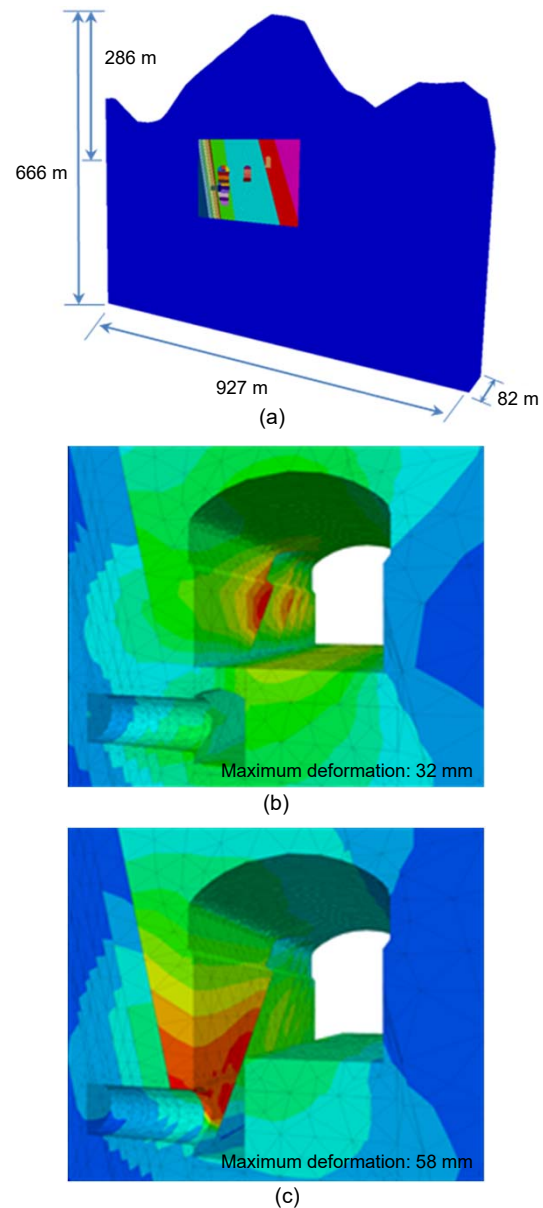


Fig. 10 Calculation model and the displacement distribution of the upstream sidewall before and after excavation of the L3 construction adit (Feng et al., 2015): (a) numerical model; (b) before excavation; (c) after excavation

fore, a series of measures can be taken in relation to the construction organization and management, excavation scheme, blasting control, support optimization design, and dynamic feedback analysis to ensure the stability of the HSBT zone in the small-angle tunnel section during construction. Based on the analysis of the abnormal deformation mechanism of the HSBT zone, composite support is adopted, such as adding anchor cables and filling grouting. At the same time,

the further development of the upstream sidewall deformation of the unit section is successfully restrained by using the information construction technology to guide the optimization of the subsequent excavation scheme. Specific measures are as follows:

Firstly, measures should be taken to increase anchor cables, such as adding a row of pre-stressed anchor cables with $T=2000$ kN per 6.0 m at 828.30, 823.80, 819.30, and 814.80 m from chainage 1+214.5 to chainage 1+316.5 (hydraulic turbine sets 7–9) of the main powerhouse. The locking value is 1700 kN, and the length of the new anchor cable is 35 m at elevations of 828.30 and 819.30 m, and 30 m for the rest.

Secondly, seam filling grouting is adopted. All the newly added anchor cable holes and the newly added seam filling grouting holes in the second drainage corridor on the upstream side of the main powerhouse are used for seam filling grouting to enhance the cohesive force of the layer and the overall strength of the rock mass. The grouting is divided from deep to shallow with a grouting hole diameter of 91 mm, a grouting depth of 20 m, and grouting pressures of 0.3–0.6 MPa. The water-cement ratios of grout are 2:1, 1:1, and 0.5:1, and the grout is transformed step by step from thin to thick. Heave deformation observation was used during grouting.

Finally, real-time monitoring of the HSBT zone's deformation and dynamic optimization of the

rock mass excavation scheme of the L3 construction branch at hydraulic turbine sets 7 and 8 are performed through the above trinity of comprehensive monitoring of rock deformation and failure, 3D fine numerical simulation, and real-time on-site feedback analysis. The two-sequence excavation and support are adopted, and each sequence is divided into three sections, with the length of each excavation and support section being about 20 m. The two-sequence excavation and support construction will start after the excavation and support construction of the adjacent first-sequence range is completed. In each region where the rock mass thickness is more than 5 m, the thin-layer excavation method is adopted to perform the excavation construction in two layers.

With these measures, the excavation and support of the construction of the right-bank main powerhouse layer VI have been completed smoothly. The deformation monitoring data show that (Fig. 11) no large deformation of the upstream high sidewall

Table 5 Factors affecting the deformation of the surrounding rock in the large underground caverns

Parameter	Value
Rock mass	
Density (kg/m^3)	2740
Bulk modulus (GPa)	8.4
Shear modulus (GPa)	5.0
Cohension (MPa)	8.0
Internal friction angle ($^\circ$)	45
Dilatancy angle ($^\circ$)	5
Tensile strength (MPa)	1.0
Structural surface	
Normal stiffness (GPa/m)	5.0
Shear stiffness (GPa/m)	1.0
Cohesion (MPa)	0.1
Frictional angle ($^\circ$)	35
Dilatancy angle ($^\circ$)	2
Residual cohesion (MPa)	0.05
Internal friction angle ($^\circ$)	20
Tensile strength (kPa)	1.0

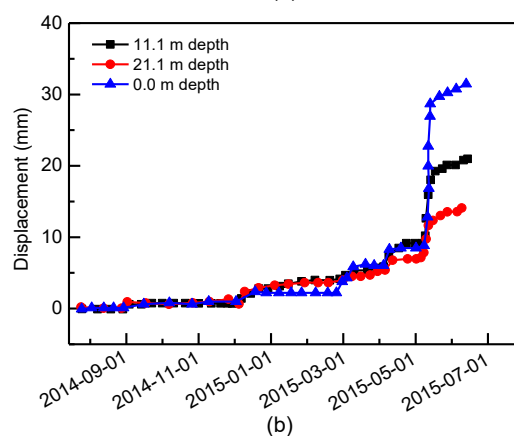
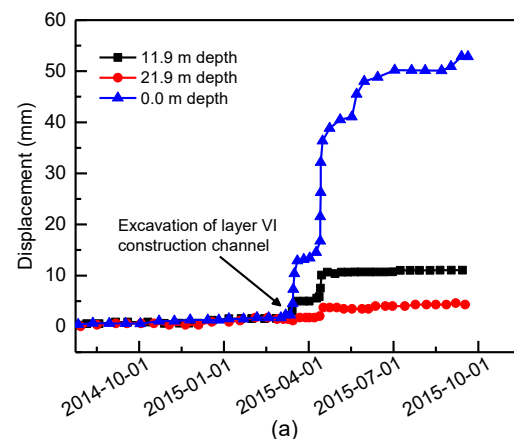


Fig. 11 Monitoring data from a multi-point displacement meter of the upstream sidewall at an elevation of 812 m: (a) No. 7 hydraulic turbine set; (b) No. 8 hydraulic turbine set

occurred in the subsequent excavation. In Fig. 11, the presented displacement value is the single value monitored by the multi-point displacement meter. Although a sudden increase of surrounding rock deformation occurred during blasting and excavation, it tended to converge after subsequent time-dependent deformation, and there was no apparent sudden increase of deformation in the abnormal parts.

5 Conclusions

Integrated theoretical analysis, numerical simulation, and case analyses were used to study the deformation characteristics and control technology of HSBT zones of large underground hydro-powerhouses. The main conclusions drawn are as follows:

(1) For the engineering excavation process of HSBT zones of a large underground powerhouse, the rapid deformation of the rock mass results from the change from a high confining pressure environment to a low confining pressure and high-stress difference conditions subjected to high in-situ stress, and the spatial effect of surrounding rock disturbance that is dominated by significant age deformation.

(2) Proper excavation and construction procedures, fine blasting control, composite and timely support, and real-time monitoring and dynamic feedback are effective technologies to ensure the stability of the surrounding rock mass of the HSBT zones.

(3) The coordinated deformation control technologies for the HSBT zones have successfully solved the spatio-temporal mismatch problem between the supports and deformations, and have been implemented at the Wudongde large underground powerhouses.

The proposed technologies can provide countermeasures for the deformation control of the high side-wall and underground tunnel groups subjected to high site stress and high seismic intensity in high-altitude regions. However, some issues can be further studied to further improve the proposed technologies and thus extend their application to other similar projects. Future research can be carried out on the following aspects:

(1) Control requirements for surrounding rock deformation in large underground caverns. This paper established the control requirements for surrounding rock deformation in the Baihetan underground power-

house. However, control requirements of universal application have not been presented because there are too many factors affecting those values. To ensure the safety and stability of a large underground powerhouse, it is necessary to establish the surrounding rock deformation control standard.

(2) Establishment of the damage models of HSBT zones. More cases need to be analyzed and summarized to obtain the failure characteristics and damage models of HSBT zones under different geological conditions. The engineering construction sequence, procedure, speed, and reinforcement technology can then be optimized.

(3) Research and development of automatic warning and support system. The automatic warning and support system for the HSBT zones can provide timely and accurate reminders to engineering personnel to carry out support and follow-up construction. This will help to avoid the phenomena of rock fragmentation and swelling, as well as concrete cracking, and greatly reduce the safety risks of excavation of the underground caverns.

Acknowledgments

This work is supported by the National Natural Science Foundation of China (Nos. 51979146 and 12102230), the China Three Gorges Corporation Research Program (Nos. WDD/0490, WDD/0578, and BHT/0774), and the China Postdoctoral Science Foundation (No. 2022M711862). The authors are very grateful to Prof. Yun-min CHEN and Dr. Duan-yang ZHUANG (Zhejiang University, China) for their critical suggestions on the research designing.

Author contributions

Qi-xiang FAN designed the research and organized the manuscript. Zhi-yun DENG and Peng LIN processed the corresponding data and edited the manuscript. Guo LI, Ji-lin FU, and Wei HE revised and edited the final version.

Conflict of interest

Qi-xiang FAN, Zhi-yun DENG, Peng LIN, Guo LI, Ji-lin FU, and Wei HE declare that they have no conflict of interest.

References

- Behnia M, Seifabad MC, 2018. Stability analysis and optimization of the support system of an underground powerhouse cavern considering rock mass variability. *Environmental Earth Sciences*, 77(18):645.
<https://doi.org/10.1007/s12665-018-7835-2>
- Broch E, 2016. Planning and utilisation of rock caverns and

- tunnels in Norway. *Tunnelling and Underground Space Technology*, 55:329-338.
<https://doi.org/10.1016/j.tust.2015.08.010>
- Chen BR, Feng XT, Huang SL, et al., 2011. Spatial-temporal feature of stress field evolution for Jinping II marble excavation in high stress zone. *Materials Research Innovations*, 15(S1):S535-S538.
<https://doi.org/10.1179/143307511x12858957676470>
- Chen F, He C, Deng JH, 2015. Concept of high geostress and its qualitative and quantitative definitions. *Rock and Soil Mechanics*, 36(4):971-980 (in Chinese).
<https://doi.org/10.16285/j.rsm.2015.04.009>
- Chen YF, Zheng HK, Wang M, et al., 2015. Excavation-induced relaxation effects and hydraulic conductivity variations in the surrounding rocks of a large-scale underground powerhouse cavern system. *Tunnelling and Underground Space Technology*, 49:253-267.
<https://doi.org/10.1016/j.tust.2015.05.007>
- Dadashi E, Noorzad A, Shahriar K, et al., 2017. Hydro-mechanical interaction analysis of reinforced concrete lining in pressure tunnels. *Tunnelling and Underground Space Technology*, 69:125-132.
<https://doi.org/10.1016/j.tust.2017.06.006>
- Dai F, Li B, Xu NW, et al., 2016. Deformation forecasting and stability analysis of large-scale underground powerhouse caverns from microseismic monitoring. *International Journal of Rock Mechanics and Mining Sciences*, 86:269-281.
<https://doi.org/10.1016/j.ijrmms.2016.05.001>
- Deng ZY, Liang NH, Liu XR, et al., 2021. Analysis and application of friction calculation model for long-distance rock pipe jacking engineering. *Tunnelling and Underground Space Technology*, 115:104063.
<https://doi.org/10.1016/j.tust.2021.104063>
- Deng ZY, Liu XR, Zhou XH, et al., 2022. Main engineering problems and countermeasures in ultra-long-distance rock pipe jacking project: water pipeline case study in Chongqing. *Tunnelling and Underground Space Technology*, 123:104420.
<https://doi.org/10.1016/j.tust.2022.104420>
- Dong JY, Yang JH, Yang GX, et al., 2011. Analysis on causes of deformation and failure of large scale underground powerhouse. *Applied Mechanics and Materials*, 71-78: 644-650.
<https://doi.org/10.4028/www.scientific.net/amm.71-78.644>
- Fan QX, Wang YF, 2010. Stability analysis of layered surrounding rock mass of large underground powerhouse of Xiangjiaba hydropower station. *Chinese Journal of Rock Mechanics and Engineering*, 29(7):1307-1313 (in Chinese).
- Fan QX, Wang YF, 2011. A case study of rock mass engineering of underground powerhouse at Xiluodu hydropower station. *Chinese Journal of Rock Mechanics and Engineering*, 30(S1):2986-2993 (in Chinese).
- Fan QX, Liu YY, Wang Y, 2011. Construction and monitoring study of large underground powerhouse caverns of Xiangjiaba hydropower station. *Chinese Journal of Rock Mechanics and Engineering*, 30(4):666-676 (in Chinese).
- [https://doi.org/1000-6915\(2011\)04-0666-11](https://doi.org/1000-6915(2011)04-0666-11)
- Fan QX, Zhou SW, Li BF, 2012a. Key technologies of rock engineering for construction of Xiluodu superhigh arch dam. *Chinese Journal of Rock Mechanics and Engineering*, 31(10):1998-2015 (in Chinese).
<https://doi.org/10.3969/j.issn.1000-6915.2012.10.005>
- Fan QX, Liu YY, Yi Z, 2012b. Key technology of tailrace system at Xiangjiaba right-bank underground powerhouse. *Chinese Journal of Rock Mechanics and Engineering*, 31(12):2377-2388 (in Chinese).
<https://doi.org/10.3969/j.issn.1000-6915.2012.12.001>
- Fan QX, Li Y, Wang HB, et al., 2018. Discussion on ventilation technique during construction of ultra-large underground caverns for Baihetan hydropower station. *Water Resources and Hydropower Engineering*, 49(9):110-119 (in Chinese).
<https://doi.org/10.13928/j.cnki.wrahe.2018.09.015>
- Fan QX, Lin P, Jiang S, et al., 2020. Review on the rock mechanics and engineering practice for large hydropower stations along the downstream section of the Jinsha river. *Journal of Tsinghua University (Science and Technology)*, 60(7):537-556 (in Chinese).
<https://doi.org/10.16511/j.cnki.qhdxxb.2020.26.011>
- Fan QX, Lin P, Wei PC, et al., 2021a. Intelligent construction of hydraulic engineering in high altitude areas: challenges and strategies. *Journal of Hydraulic Engineering*, 52(12):1404-1417 (in Chinese).
<https://doi.org/10.13243/j.cnki.slxb.20210320>
- Fan QX, Wang ZL, He W, et al., 2021b. Technological innovations in construction of underground caverns in basaltic rocks at Baihetan hydropower station on Jinsha river. *Scientia Sinica Technologica*, 51(9):1088-1106 (in Chinese).
<https://doi.org/10.1360/sst-2021-0053>
- Feng X, Xu D, Chen D, et al., 2015. Discrete Element Analysis of Stability of Surrounding Rock of Upstream Side Wall of 7#~8# Unit Section of Right Bank Main Powerhouse. Report No. IRSM-IRM-WDDDC-15, Institute of Rock and Soil Mechanics, Chinese Academy of Sciences, Wuhan, China (in Chinese).
- Gan DQ, Yang X, Zhang YP, et al., 2019. Stability analysis of underground multicavities in bench blasting vibration. *Mathematical Problems in Engineering*, 2019:4014761.
<https://doi.org/10.1155/2019/4014761>
- Ghorbani M, Sharifzadeh M, 2009. Long term stability assessment of Siah Bisheh powerhouse cavern based on displacement back analysis method. *Tunnelling and Underground Space Technology*, 24(5):574-583.
<https://doi.org/10.1016/j.tust.2009.02.007>
- Han G, Zhou H, Chen JL, et al., 2019. Engineering geological properties of interlayer staggered zones at Baihetan hydropower station. *Rock and Soil Mechanics*, 40(9):3559-3568 (in Chinese).
<https://doi.org/10.16285/j.rsm.2018.1251>
- Hoek E, Brown ET, 1980. *Underground Excavations in Rock*. CRC Press, Boca Raton, USA, p.527.
- Hoek E, Carranza-Torres C, Corkum B, 2002. Hoek-Brown

- Failure Criterion–2002 Edition.
<https://static.rocscience.cloud/assets/verification-and-theory/RSDData/Hoek-Brown-Failure-Criterion-2002-Edition.pdf>
- Hoek E, Carter TG, Diederichs MS, 2013. Quantification of the geological strength index chart. Proceedings of the 47th U.S. Rock Mechanics/Geomechanics Symposium, p.1757-1764.
- Hu ZH, Xu NW, Dai F, et al., 2018. Stability and deformation mechanism of bedding rock masses at the underground powerhouse of Wudongde hydropower station. *Rock and Soil Mechanics*, 39(10):3794-3802 (in Chinese).
<https://doi.org/10.16285/j.rsm.2017.0293>
- Hu ZH, Xu NW, Li B, et al., 2020. Stability analysis of the arch crown of a large-scale underground powerhouse during excavation. *Rock Mechanics and Rock Engineering*, 53(6):2935-2943.
<https://doi.org/10.1007/s00603-020-02077-4>
- Huang JH, Luo Y, Zhang G, et al., 2022. Numerical analysis on rock blasting damage in Xiluodu underground powerhouse using an improved constitutive model. *European Journal of Environmental and Civil Engineering*, 26(7): 3009-3026.
<https://doi.org/10.1080/19648189.2020.1780475>
- Huang SL, Ding XL, Zhang YT, et al., 2020. Field and numerical investigation of high wall stability with thin, steeply dipping strata in an underground powerhouse. *International Journal of Geomechanics*, 20(6):04020055.
[https://doi.org/10.1061/\(asce\)gm.1943-5622.0001685](https://doi.org/10.1061/(asce)gm.1943-5622.0001685)
- Ishida T, Kanagawa T, Uchita Y, 2014. Acoustic emission induced by progressive excavation of an underground powerhouse. *International Journal of Rock Mechanics and Mining Sciences*, 71:362-368.
<https://doi.org/10.1016/j.ijrmms.2014.08.001>
- Jiang Q, Feng XT, Fan YL, et al., 2017. In situ experimental investigation of basalt spalling in a large underground powerhouse cavern. *Tunnelling and Underground Space Technology*, 68:82-94.
<https://doi.org/10.1016/j.tust.2017.05.020>
- Jiang Q, Feng XT, Li SJ, et al., 2019. Cracking-restraint design method for large underground caverns with hard rock under high geostress condition and its practical application. *Chinese Journal of Rock Mechanics and Engineering*, 38(6):1081-1101 (in Chinese).
<https://doi.org/10.13722/j.cnki.jrme.2018.1147>
- Jiang RC, Dai F, Liu Y, et al., 2020. An automatic classification method for microseismic events and blasts during rock excavation of underground caverns. *Tunnelling and Underground Space Technology*, 101:103425.
<https://doi.org/10.1016/j.tust.2020.103425>
- Jiang X, Xu NW, Zhou Z, et al., 2019. Failure mechanism of surrounding rock of bus-bar tunnels at Lianghekou hydropower station subjected to excavation. *Rock and Soil Mechanics*, 40(1):305-314 (in Chinese).
<https://doi.org/10.16285/j.rsm.2017.1206>
- Jin CY, Ma ZY, Zhang YL, 2009. Prediction of surrounding deformations of underground powerhouse using ANFIS. *Journal of Dalian University of Technology*, 49(4): 576-579 (in Chinese).
<https://doi.org/10.7511/dllgxb200904019>
- Jing MG, Zhu L, Liu KP, et al., 2015. Study of blasting excavation of Nanganqu hydraulic tunnel in Xiangjiaba hydropower station. *Blasting*, 32(3):133-138 (in Chinese).
<https://doi.org/10.3963/j.issn.1001-487X.2015.03.024>
- Kumar K, Saini RP, 2022. A review on operation and maintenance of hydropower plants. *Sustainable Energy Technologies and Assessments*, 49:101704.
<https://doi.org/10.1016/j.seta.2021.101704>
- Kumar V, Jha PC, Singh NP, et al., 2021. Dynamic stability evaluation of underground powerhouse cavern using microseismic monitoring. *Geotechnical and Geological Engineering*, 39(3):1795-1815.
<https://doi.org/10.1007/s10706-020-01588-9>
- Li B, Dai F, Xu NW, et al., 2013. Establishment and application of microseismic monitoring system to deep-buried underground powerhouse. *Advanced Materials Research*, 838-841:889-893.
<https://doi.org/10.4028/www.scientific.net/AMR.838-841.889>
- Li HB, Yang XG, Zhang XB, et al., 2017. Deformation and failure analyses of large underground caverns during construction of the Houziyan hydropower station, Southwest China. *Engineering Failure Analysis*, 80:164-185.
<https://doi.org/10.1016/j.engfailanal.2017.06.037>
- Li X, Li YL, Zhang P, et al., 2017. Precision analysis of seepage monitoring optimization mathematical model for dam body of Pubugou hydropower station. *Water Resources and Power*, 35(12):55-57 (in Chinese).
- Li XP, Lv JL, Luo Y, et al., 2018. Mechanism study on elevation effect of blast wave propagation in high side wall of deep underground powerhouse. *Shock and Vibration*, 2018:4951948.
<https://doi.org/10.1155/2018/4951948>
- Li XP, Bian X, Luo Y, et al., 2020. Study on attenuation law of blasting vibration propagation of side wall of underground cavern. *Rock and Soil Mechanics*, 41(6): 2063-2069 (in Chinese).
<https://doi.org/10.16285/j.rsm.2019.1009>
- Li Y, Zhu WS, Fu JW, et al., 2014. A damage rheology model applied to analysis of splitting failure in underground caverns of Jinping I hydropower station. *International Journal of Rock Mechanics and Mining Sciences*, 71: 224-234.
<https://doi.org/10.1016/j.ijrmms.2014.04.027>
- Lin P, Wang RK, Kang SZ, et al., 2011. Key problems of foundation failure, reinforcement and stability for super-high arch dams. *Chinese Journal of Rock Mechanics and Engineering*, 30(10):1945-1958 (in Chinese).
- Lin P, Zhou YN, Liu HY, et al., 2013. Reinforcement design and stability analysis for large-span tailrace bifurcated tunnels with irregular geometry. *Tunnelling and Underground Space Technology*, 38:189-204.
<https://doi.org/10.1016/j.tust.2013.07.011>
- Lin P, Liu HY, Zhou WY, 2015. Experimental study on failure behaviour of deep tunnels under high in-situ stresses. *Tunnelling and Underground Space Technology*, 46:28-45.
<https://doi.org/10.1016/j.tust.2014.10.009>
- Lin P, Shi J, Wei PC, et al., 2019. Shallow unloading deformation

- analysis on Baihetan super-high arch dam foundation. *Bulletin of Engineering Geology and the Environment*, 78(8):5551-5568.
<https://doi.org/10.1007/s10064-019-01484-4>
- Liu W, 2010. Construction technology of twice tensioning for high-strength prestressed anchor bolt for rock-wall crane beam in underground powerhouse of Pengshui hydro-power station. *Water Resources and Hydropower Engineering*, 41(7):57-59 (in Chinese).
<https://doi.org/10.3969/j.issn.1000-0860.2010.07.015>
- Lu JJ, Fang D, Li LQ, 2018. Optimal design of supporting for underground powerhouse on left bank of Baihetan hydro-power station. *Water Resources and Hydropower Engineering*, 49(8):128-135 (in Chinese).
<https://doi.org/10.13928/j.cnki.wrahe.2018.08.017>
- Luo DN, Lin P, Li QB, et al., 2015. Effect of the impounding process on the overall stability of a high arch dam: a case study of the Xiluodu dam, China. *Arabian Journal of Geosciences*, 8(11):9023-9041.
<https://doi.org/10.1007/s12517-015-1868-6>
- Luo ST, Yang FJ, Zhou H, et al., 2020. Multi-index prediction method for maximum convergence deformation of underground powerhouse side wall based on statistical analysis. *Rock and Soil Mechanics*, 41(10): 3415-3424 (in Chinese).
<https://doi.org/10.16285/j.rsm.2020.0062>
- Lv XL, Chi SC, 2018. Strain analysis of the Nuozhadu high rockfill dam during initial impoundment. *Mathematical Problems in Engineering*, 2018:7291473.
<https://doi.org/10.1155/2018/7291473>
- Ma K, Zhang JH, Zhou Z, et al., 2020. Comprehensive analysis of the surrounding rock mass stability in the underground caverns of Jinping I hydropower station in Southwest China. *Tunnelling and Underground Space Technology*, 104:103525.
<https://doi.org/10.1016/j.tust.2020.103525>
- Menéndez J, Schmidt F, Konietzky H, et al., 2019. Stability analysis of the underground infrastructure for pumped storage hydropower plants in closed coal mines. *Tunnelling and Underground Space Technology*, 94:103117.
<https://doi.org/10.1016/j.tust.2019.103117>
- MWR (Ministry of Water Resources of the People's Republic of China), 2014. Design Code for Hydropower House, SL 266-2014. MWR, Beijing, China (in Chinese).
- Panthi KK, Broch E, 2022. Underground hydropower plants. *Comprehensive Renewable Energy*, 6:126-146.
<https://doi.org/10.1016/B978-0-12-819727-1.00077-7>
- Pinheiro M, Emery X, Miranda T, et al., 2021. Using geotechnical scenarios for underground structure analysis: a case study in a hydroelectric complex in northern Portugal. *Tunnelling and Underground Space Technology*, 111: 103855.
<https://doi.org/10.1016/j.tust.2021.103855>
- Rezaei M, Rajabi M, 2018. Vertical displacement estimation in roof and floor of an underground powerhouse cavern. *Engineering Failure Analysis*, 90:290-309.
<https://doi.org/10.1016/j.engfailanal.2018.03.010>
- Shen JY, Priest SD, Karakus M, 2012. Determination of Mohr–Coulomb shear strength parameters from generalized Hoek–Brown criterion for slope stability analysis. *Rock Mechanics and Rock Engineering*, 45(1):123-129.
<https://doi.org/10.1007/s00603-011-0184-z>
- Shi AC, Li CJ, Hong WB, et al., 2022. Comparative analysis of deformation and failure mechanisms of underground powerhouses on the left and right banks of Baihetan hydropower station. *Journal of Rock Mechanics and Geotechnical Engineering*, 14(3):731-745.
<https://doi.org/10.1016/j.jrmge.2021.09.012>
- Shi J, Lin P, Zhou YD, et al., 2018. Reinforcement analysis of toe blocks and anchor cables at the Xiluodu super-high arch dam. *Rock Mechanics and Rock Engineering*, 51(8): 2533-2554.
<https://doi.org/10.1007/s00603-018-1517-y>
- Song SW, Feng XM, Liao CG, et al., 2016. Measures for controlling large deformations of underground caverns under high in-situ stress condition—a case study of Jinping I hydropower station. *Journal of Rock Mechanics and Geotechnical Engineering*, 8(5):605-618.
<https://doi.org/10.1016/j.jrmge.2016.06.002>
- Sun H, Du WS, Liu C, 2021. Uniaxial compressive strength determination of rocks using X-ray computed tomography and convolutional neural networks. *Rock Mechanics and Rock Engineering*, 54(8):4225-4237.
<https://doi.org/10.1007/s00603-021-02503-1>
- Sun YP, Li B, Dong LL, et al., 2021. Microseismic moment tensor based analysis of rock mass failure mechanism surrounding an underground powerhouse. *Geomatics, Natural Hazards and Risk*, 12(1):1315-1342.
<https://doi.org/10.1080/19475705.2021.1918266>
- Wang M, Li HB, Han JQ, et al., 2019. Large deformation evolution and failure mechanism analysis of the multi-freeface surrounding rock mass in the Baihetan underground powerhouse. *Engineering Failure Analysis*, 100:214-226.
<https://doi.org/10.1016/j.engfailanal.2019.02.056>
- Wang M, Zhou JW, Shi AC, et al., 2020. Key factors affecting the deformation and failure of surrounding rock masses in large-scale underground powerhouses. *Advances in Civil Engineering*, 2020:8843466.
<https://doi.org/10.1155/2020/8843466>
- Wang Q, Shao L, 2010. Stability analysis of Nuozhadu rock-fill dam based on non-circular slip surface. *Water Resources and Power*, 28(10):56-58 (in Chinese).
<https://doi.org/10.3969/j.issn.1000-7709.2010.10.019>
- Wang ZS, Li Y, Zhu WS, et al., 2016. Splitting failure in side walls of a large-scale underground cavern group: a numerical modelling and a field study. *SpringerPlus*, 5(1):1528.
<https://doi.org/10.1186/s40064-016-3214-1>
- Wen LF, Li YL, Chai JR, 2020. Numerical simulation and performance assessment of seepage control effect on the fractured surrounding rock of the Wunonglong underground powerhouse. *International Journal of Geomechanics*, 20(12):05020006.
[https://doi.org/10.1061/\(asce\)gm.1943-5622.0001879](https://doi.org/10.1061/(asce)gm.1943-5622.0001879)
- Wu AQ, Wang JM, Zhou Z, et al., 2016. Engineering rock mechanics practices in the underground powerhouse at

- Jinping I hydropower station. *Journal of Rock Mechanics and Geotechnical Engineering*, 8(5):640-650.
<https://doi.org/10.1016/j.jrmge.2016.05.001>
- Wu FQ, Hu XH, Gong MF, et al., 2010. Unloading deformation during layered excavation for the underground powerhouse of Jinping I hydropower station, Southwest China. *Bulletin of Engineering Geology and the Environment*, 69(3):343-351.
<https://doi.org/10.1007/s10064-010-0308-9>
- Xiao PW, Li TB, Xu NW, et al., 2019. Microseismic monitoring and deformation early warning of the underground caverns of Lianghekou hydropower station, Southwest China. *Arabian Journal of Geosciences*, 12(16):496.
<https://doi.org/10.1007/s12517-019-4683-7>
- Xiao YX, Feng XT, Feng GL, et al., 2016. Mechanism of evolution of stress-structure controlled collapse of surrounding rock in caverns: a case study from the Baihetan hydropower station in China. *Tunnelling and Underground Space Technology*, 51:56-67.
<https://doi.org/10.1016/j.tust.2015.10.020>
- Zhang CH, Zhang YL, 2009. Nonlinear dynamic analysis of the Three Gorge project powerhouse excited by pressure fluctuation. *Journal of Zhejiang University-SCIENCE A*, 10(9):1231-1240.
<https://doi.org/10.1631/jzus.A0820478>
- Zhang JH, Wang RK, Zhou Z, et al., 2018. Pre-load factor of the pre-stressed anchor cable in underground powerhouse with high geo-stress. *Rock and Soil Mechanics*, 39(3):1002-1008 (in Chinese).
<https://doi.org/10.16285/j.rsm.2016.0751>
- Zhang QY, Li F, Duan K, et al., 2021. Experimental investigation on splitting failure of high sidewall cavern under three-dimensional high in-situ stress. *Tunnelling and Underground Space Technology*, 108:103725.
<https://doi.org/10.1016/j.tust.2020.103725>
- Zhou YY, Xu DP, Gu GK, et al., 2019. The failure mechanism and construction practice of large underground caverns in steeply dipping layered rock masses. *Engineering Geology*, 250:45-64.
<https://doi.org/10.1016/j.enggeo.2019.01.006>
- Zhu WS, Sun AH, Wang WT, et al., 2007. Study on prediction of high wall displacement and stability judging method of surrounding rock for large cavern groups. *Chinese Journal of Rock Mechanics and Engineering*, 26(9): 1729-1736 (in Chinese).
<https://doi.org/10.3321/j.issn:1000-6915.2007.09.001>
- Zhu WS, Li XJ, Zhang QB, et al., 2010. A study on sidewall displacement prediction and stability evaluations for large underground power station caverns. *International Journal of Rock Mechanics and Mining Sciences*, 47(7): 1055-1062.
<https://doi.org/10.1016/j.ijrmms.2010.07.008>